

On Discrete Time Optimal Control: A Closed-Form Solution

Zhiqiang Gao
Center for Advanced Control Technologies
Cleveland State University,
Cleveland, OH 44115
z.gao@csuohio.edu

Abstract: In this paper, the mathematical derivation of a closed-form discrete optimal control law is presented. Unlike the well-known results for continuous plants, the closed-form time optimal control for discrete time plants was never attained. The recent work of Jingqing Han sheds lights on this problem and is introduced. In particular, a time optimal control law is constructed in the form of state feedback for a discrete time, double-integral plant by using the Isochronic Region method. This closed-form nonlinear state feedback clearly demonstrates that time optimal control in discrete time is not necessarily bang-bang control, i.e., the control signal does not always take on extreme values. In fact, this characteristic makes the new control law advantageous in engineering applications.

Keywords: Time Optimal Control, Bang-Bang Control, Discrete Time Optimal Control.

I. INTRODUCTION

Time optimal control (TOC) originated from servo control design problems [1,2] in the 50s, where heuristic arguments were made regarding the optimality. It was extended to a standard second-order system $\ddot{y} + 2\zeta \dot{y} + y = \varphi(y, \dot{y})$, where $\varphi(y, \dot{y})$ is a switching function of values ± 1 [3]. This problem drew significant interests in the field of applied mathematics which gave birth to Optimal Control Theory [4-7]. In particular, Pontryagin's minimum principle [4] greatly simplified the derivation of time optimal control law, which was previously quite cumbersome. Furthermore, based on this principle, the existence of a solution, the uniqueness of the solution and the number of switches in control signal were proved for time optimal control of a linear, time-invariant continuous plant. That is, $\dot{x}(t) = Ax(t) + Bu(t)$, where A and B are constant $n \times n$ and $n \times m$ matrices, respectively, and the components of $u(t)$ are constrained by $|u_i(t)| \leq 1$.

From an engineering perspective, the applications of TOC prove to be challenging. A nagging problem is that the instant switching between extreme values in the control signal required by TOC is often neither feasible, because of the physical limits on how fast a control signal can change, nor desirable, because of the stress it puts on the control actuators. On the other hand, the research continues in development of methodology to determine switching

surfaces for various (continuous) plants. Overall, TOC still draws considerable interests in research for both practical and theoretical reasons. See, for example, recent papers and the references therein in [12,13].

With the rapid development of computer control technology, most control algorithms are implemented in discrete time domain today. Direct digitization of continuous TOC solution proves to be problematic in practice because of the high frequency chattering of the control signal. This leads to the question of whether or not a TOC solution derived directly for discrete time plants offers any advantages.

It is a well-known fact that the nonsingular time-optimal control solution of continuous linear-analytic systems with bounded control inputs is a bang-bang control. However, it was shown by Tsien and Song that time optimal control for discrete plants is not a bang-bang control [7]. They investigated this problem and gave a method for discrete time optimal control (DTOC) design, but were not able to arrive at a closed-form solution. Meanwhile, digitized bang-bang control has been used as an approximation for DTOC problems.

This leads us to the work of Jingqing Han, one of the pioneer researchers on time optimal control in the early 1960s (also known as Hang King-Ching). A significant amount of his early work in both continuous and discrete time optimal control appeared in [7]. His work in [8] was widely referenced, and his and his colleagues' work in discrete time optimal control proved to be promising [7,9]. Unfortunately, the work was interrupted by political events in China, and it was not until over thirty years later that he and his students studied this problem again. This time, they used the TOC as a means to build a nonlinear differentiator [11]. Overshoot and poor numerical properties of continuous TOC solutions led his team to seek answers in his earlier work in DTOC. And a closed-form DTOC solution for a double-integral plant was found [10].

The paper is organized as follows: the background on TOC for a continuous double integral-plant and its approximations are introduced in section II. The construction of the DTOC algorithm is introduced in section III, followed by concluding remarks in section IV.

II. BACKGROUND

Time optimal control as a research topic has been studied for over a half century by at least two generations. In this section, some early results and basic concepts are reviewed.

2.1 Continuous TOC and Its Approximations

One problem that has received considerable attention in literature is the time optimal control of the double-integral plant defined as

$$\dot{x}(t) = \begin{bmatrix} 0 & 1 \\ 0 & 0 \end{bmatrix} x(t) + \begin{bmatrix} 0 \\ 1 \end{bmatrix} u(t), |u(t)| \leq r \quad (2.1)$$

where $x(t) = [x_1(t) \ x_2(t)]^T$. The resulting control law that drives the state from any initial point to the origin in minimum time is [5-8]

$$u(t) = -r \operatorname{sign}(s) \quad (2.2)$$

where the switching function is defined as

$$s = \begin{cases} x_1(t) + \frac{x_2(t)|x_2(t)|}{2r} & x_1(t) + \frac{x_2(t)|x_2(t)|}{2r} \neq 0 \\ x_2(t) & x_1(t) + \frac{x_2(t)|x_2(t)|}{2r} = 0 \\ 0 & x_1(t) + \frac{x_2(t)|x_2(t)|}{2r} = 0 \end{cases} \quad x(t) \neq 0 \quad (2.3)$$

and the sign function, $\operatorname{sign}(s)$, is defined, for a scalar s , as

$$\operatorname{sign}(s) = \begin{cases} 1 & s > 0 \\ 0 & s = 0 \\ -1 & s < 0 \end{cases} \quad (2.4)$$

Note that in the implementation of this algorithm, the conditions

$$x(t) = 0 \text{ and } x_1(t) + \frac{x_2(t)|x_2(t)|}{2r} = 0 \quad (2.5)$$

were hardly ever met in a noisy environment. Therefore, the time optimal control law is often simplified as

$$u(t) = -r \operatorname{sign}\left(x_1(t) + \frac{x_2(t)|x_2(t)|}{2r}\right) \quad (2.6)$$

This time optimal control method has many advantages over linear controllers: 1) the state arrives at the steady state in minimal and finite time; 2) superior disturbance rejection robustness against dynamic uncertainties. It can also be easily extended to the tracking problem by replacing $x_1(t)$ and $x_2(t)$ in (2.3) with $x_1(t) - v(t)$ and $x_2(t) - \dot{v}(t)$, respectively. Here $v(t)$ and $\dot{v}(t)$ are the desired state trajectories.

In many engineering control applications, one of the design goals is to achieve maximum bandwidth, which is a term derived from linear transfer functions. In time domain, it corresponds to maximum accuracy in command following and minimal disturbance recovery time. In this sense, the time optimal controller has a higher bandwidth than any other controllers, linear or nonlinear.

The penalty associated with this control law is the frequent switching of the control signal between its two extreme values around the switching curve described in (2.5), particularly around the origin, $x=0$. Furthermore, the instant switching requires an infinitely large du/dt , which is usually not practical. Many modifications of the control law (2.2) were made to ease the implementation:

- Adding a dead zone or a linear zone:

$$u = 0, \text{ if } \|x\| < \delta \quad (2.7)$$

can be added to (2.2) to reduce the chattering of u around the origin. δ can be chosen by trial and error or set to

$$\delta = \|n\|_\infty \quad (2.8)$$

where n is the measurement noise in x . Or,

$$u = k_1 x_1 + k_2 x_2, \text{ if } \|x\| < \delta \quad (2.9)$$

where k_1 and k_2 are linear gains to be selected.

- Replacing $\operatorname{sign}(s)$ in (2.2) with

$$\operatorname{sat}(s, \delta) = \begin{cases} \operatorname{sign}(s) & s > \delta \\ \frac{s}{\delta} & |s| \leq \delta \end{cases} \quad (2.10)$$

It seems this modification should only occur around the origin.

- Keeping u unchanged in the neighborhood of the switching curve s in (2.5), defined as the area borders by, for example, the two curves

$$(x_1(t) \pm \lambda) + \frac{x_2(t)|x_2(t)|}{2r} = 0, \lambda > 0 \quad (2.11)$$

These modifications make the solution suboptimal. They reflect the need to make a compromise in design between the performance (optimality) and the physical constraints (du/dt , number of switches, etc.)

2.2 Discrete TOC and Isochronic Regions

Consider a discrete time double-integral plant

$$x(k+1) = Ax(k) + Bu(k), |u(k)| \leq r \quad (2.12)$$

$$\text{where } A = \begin{bmatrix} 1 & h \\ 0 & 1 \end{bmatrix} \text{ and } B = \begin{bmatrix} 0 \\ h \end{bmatrix}$$

The interest here is to find a time optimal control law directly in discrete time domain. This problem is defined as follows:

Definition 1: Given the plant (2.12) and its initial state $x(0)$, determining the control signal sequence, $u(0), u(1), \dots, u(k)$, such that the state $x(k)$ is driven back to the origin in a minimum number of steps, subject to the constraint of $|u(k)| \leq r$. i.e.

$$\text{find } u(k^*), |u(k)| \leq r, \text{ such that } k^* = \min\{k | x(k) = 0\} \quad (2.13)$$

Note that an open loop solution to (2.13) is the one where $u(i)$, $i=1, \dots, k$, is solely dependent only on the initial condition, $x(0)$. Because such a solution does not take into consideration the disturbances in the plant, it is not a practical one. The closed-loop solution is the one where u is a function of the state, x . In a discrete time control

system, the state is measured only at the sampling instant, $t=kh$, where h is the sampling period. If we treat the measurement, $x(kh)$, as though it is an initial condition, $x(0)$, then all we need to find is $u(0)$ in (2.13) at each sampling instant. Repeat it until the state reaches the origin. This approach is used in the following in deriving the discrete time optimal control law (DTCOL).

Definition 2: Isochronic Region (IR) $G(k)$ denotes the set of states that, for any $x(0) \in G(k)$, there is at least one admissible control sequence, $u(0), u(1), \dots, u(k)$, which makes the solution of (2.12) satisfy $x(k)=0$.

Strategy

Note that the IR grows in volumes as k increases, i.e., $G(k-1) \in G(k)$. The basic idea in deriving the DTCOL is to find $u(0)$ for any $x(0) \in G(k)$ and $x(0) \notin G(k-1)$, such that the next state $x(1)$, calculated from (2.1), satisfies $x(1) \in G(k-1)$. This process is divided into two tasks:

1. Determine $G(k)$, i.e., the representation of the initial condition, $x(0)$, in terms of h and r , from which the state can be driven back to the origin in k steps;
2. For any given initial condition $x(0)$, find the corresponding $u(0)$ as a function of $x(0)$, where $u(0)$ is the first step in (2.13).

First, let's examine $G(k)$. From (2.12),

$$\begin{aligned} x(1) &= Ax(0) + Bu(0) \\ x(2) &= Ax(1) + Bu(1) = A^2x(0) + ABu(0) + Bu(1) \\ &\dots \end{aligned}$$

$$x(k) = A^k x(0) + A^{k-1} Bu(0) + \dots + ABu(k-2) + Bu(k-1)$$

Setting $x(k)=0$ and solve for $x(0)$, we have

$$x(0) = -A^{-1} Bu(0) - A^{-2} Bu(1) - \dots - A^{-k} Bu(k-1) \quad (2.14)$$

With $A^k = \begin{bmatrix} 1 & kh \\ 0 & 1 \end{bmatrix}$ and $A^{-k} = \begin{bmatrix} 1 & -kh \\ 0 & 1 \end{bmatrix}$, (2.14) can be

rewritten as

$$x(0) = \sum_{i=1}^k \begin{bmatrix} ih^2 \\ -h \end{bmatrix} u(i-1) \quad (2.15)$$

Clearly,

$$G(k) = \left\{ \sum_{i=1}^k \begin{bmatrix} ih^2 \\ -h \end{bmatrix} u(i-1), |u(i)| \leq r, \right\} \quad (2.16)$$

Graphical Interpretations of IR:

Consider

$$\begin{aligned} G(1) &= \left\{ \begin{bmatrix} h^2 \\ -h \end{bmatrix} u(0) \right\}, \quad G(2) = \left\{ \begin{bmatrix} h^2 \\ -h \end{bmatrix} u(0) + \begin{bmatrix} 2h^2 \\ -h \end{bmatrix} u(1) \right\}, \\ G(3) &= \left\{ \begin{bmatrix} h^2 \\ -h \end{bmatrix} u(0) + \begin{bmatrix} 2h^2 \\ -h \end{bmatrix} u(1) + \begin{bmatrix} 3h^2 \\ -h \end{bmatrix} u(2) \right\} \end{aligned} \quad (2.17)$$

Let $u(i)$ take the extreme values of r or $-r$, the resulting $G(k)$, $k=1,2,3$, is plotted below on the phase plane in Figure 2.1. Note that $G(1)$ is a straight line between

$$\{a_{.1} = \begin{bmatrix} -h^2 r \\ hr \end{bmatrix} \text{ and } a_{.1} = \begin{bmatrix} h^2 r \\ -hr \end{bmatrix}\}; \quad (2.18)$$

$G(2)$ is a parallelogram defined by the four points of

$$\{a_2 = \begin{bmatrix} 3h^2 r \\ -2hr \end{bmatrix}, a_{.2} = \begin{bmatrix} -3h^2 r \\ 2hr \end{bmatrix}, b_2 = \begin{bmatrix} -h^2 r \\ 0 \end{bmatrix}, b_{.2} = \begin{bmatrix} h^2 r \\ 0 \end{bmatrix}\} \quad (2.19)$$

$G(3)$ is a hexagon defined by the six points of

$$\begin{aligned} \{a_3 = \begin{bmatrix} 6h^2 r \\ -3hr \end{bmatrix}, a_{.3} = \begin{bmatrix} -6h^2 r \\ 3hr \end{bmatrix}, b_3 = \begin{bmatrix} -4h^2 r \\ hr \end{bmatrix}, \\ b_{.3} = \begin{bmatrix} 4h^2 r \\ -hr \end{bmatrix}, s_3 = \begin{bmatrix} 0 \\ -h^2 r \end{bmatrix}, s_{.3} = \begin{bmatrix} 0 \\ h^2 r \end{bmatrix}\} \end{aligned} \quad (2.20)$$

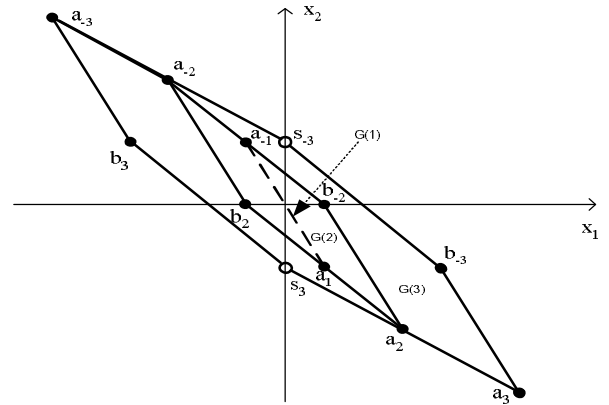


Figure 2.1 Isochronic Regions $G(1)$ to $G(3)$

III. CONSTRUCTION OF THE DISCRETE TIME OPTIMAL CONTROL LAW

In this section, the DTCOL is obtained constructively based on the IR, $G(k)$, $k=1, 2, \dots$, as defined above.

3.1 DTCOL for $G(1)$ and beyond

For any initial state in $G(k)$, a control sequence is to be found so that $x(k)=0$. For example, if $x(0)$ is on the line defined in $G(1)$, as shown in Figure 2.1, it satisfies

$$x(0) = \alpha a_{.1} + (1-\alpha) a_1 = (1-2\alpha) \begin{bmatrix} h^2 r \\ -hr \end{bmatrix}, \quad 0 < \alpha < 1, \quad (3.1)$$

then

$$x(1) = Ax(0) + Bu(0) = \begin{bmatrix} 0 \\ -(1-2\alpha)hr + hu(0) \end{bmatrix} \quad (3.2)$$

and the state can be driven back to the origin in one step by using a control signal

$$u(0) = (1-2\alpha)r = -x_2(0)/h \quad (3.3)$$

Since $G(1)$ is the straight line connecting a_1 and $a_{.1}$, it can be described by

$$|x_2(0)| \leq hr, \quad x_1(0) + hx_2(0) = 0 \quad (3.4)$$

The time optimal control law for $G(1)$ can then be written as

$$u(0) = -x_2(0)/h, \quad |x_2(0)| \leq hr, \quad x_1(0) + hx_2(0) = 0 \quad (3.5)$$

For the $x(0)$ on the same line of $G(1)$ but goes beyond the a_1 and a_{-1} points, i.e.,

$$|x_2(0)| > hr, x_1(0) + hx_2(0) = 0 \quad (3.6)$$

the DTOC calls for $u(0)$ to take on extreme values of $-r$ or r , depending on whether $x(0)$ is on the a_1 or a_{-1} side of the origin, until $x(0)$ enters $G(1)$. Therefore, the time optimal control for any $x(0)$ satisfying $x_1(0) + hx_2(0) = 0$ is

$$u(0) = -rsat(x_2(0), hr), x_1(0) + hx_2(0) = 0 \quad (3.7)$$

Consider that each measurement at the sampling instant is treated as the initial condition, the DTOCL for $G(1)$ can simply be written as

$$u = -rsat(x_2, hr), x_1 + hx_2 = 0 \quad (3.8)$$

Remark:

The DTOC law for $G(1)$ clearly demonstrates that, unlike its continuous time counterpart, the control signal, u , does not always take on the extreme value. There is an inherent linear region in DTOC law, and the size of this region is proportional to the sampling period and the maximum control magnitude.

3.2 DTOC Law for $G(2)$ and the area defined by $|y| \leq h^2 r$

For $k > 1$, such a solution is not so obvious. In the following, the problem of synthesizing a control law for $G(k)$, $k > 1$, is addressed. The objective here is to derive the DTOC law in terms of state feedback.

As shown in Figure 3.1, $G(2)$ is a parallelogram defined by points in (2.19). Note that the lines $[a_{-2}b_2]$ and $[b_{-2}a_2]$ are parallel to $[a_1a_{-1}]$. Let,

$$y = x_1 + hx_2 \quad (3.9)$$

the boundaries of this parallelogram are four straight lines described as

$$\begin{aligned} a_2 b_{-2}: y = x_1 + hx_2 = h^2 r \\ a_{-2} b_2: y = x_1 + hx_2 = -h^2 r \\ a_2 b_2: x_1 + 2hx_2 = y + hx_2 = h^2 r \\ a_{-2} b_{-2}: x_1 + 2hx_2 = y + hx_2 = -h^2 r \end{aligned} \quad (3.10)$$

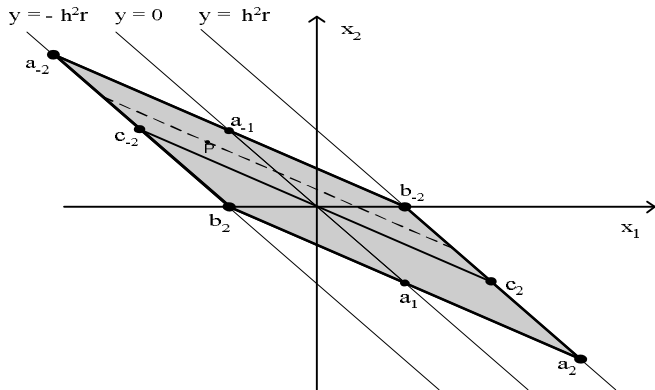


Figure 3.1 Control Law Derivation for $G(2)$

It can be easily verified that for any $x(0)$ on $a_{-2}b_2$ (a_2b_2), $u(0) = -r$ ($u(0) = r$) will always force $x(1)$ to be inside $G(1)$.

Furthermore, any point inside the parallelogram, such as P in Figure 3.1, resides on a line parallel to $a_{-2}b_2$, which satisfies

$$x_1 + 2hx_2 = y + hx_2 = (2\alpha - 1)h^2 r, \quad 0 \leq \alpha \leq 1 \quad (3.11)$$

subject to

$$\left| \frac{x_1 + 2hx_2}{h} \right| = \left| x_2 + \frac{y}{h} \right| \leq hr \quad \text{and} \quad |x_1 + hx_2| = |y| \leq h^2 r \quad (3.12)$$

Note that $\alpha = 1$ and $\alpha = 0$ correspond to $a_{-2}b_2$ and a_2b_2 , respectively. The corresponding time optimal control is

$$u(0) = -(2\alpha - 1)r = -\frac{x_1(0) + 2hx_2(0)}{h^2} = -\frac{x_2(0) + y(0)/h}{h},$$

$$\left| x_2(0) + \frac{y(0)}{h} \right| \leq hr; \quad |y(0)| \leq h^2 r \quad (3.13)$$

because it results in

$$\begin{aligned} x(1) &= \begin{bmatrix} x_1(1) \\ x_2(1) \end{bmatrix} = Ax(0) + Bu(0) = \begin{bmatrix} x_1(0) + hx_2(0) \\ x_2(0) + hu(0) \end{bmatrix} \\ &= \begin{bmatrix} y(0) \\ x_2(0) + h(-\frac{x_2(0) + y(0)/h}{h}) \end{bmatrix} = \begin{bmatrix} y(0) \\ -y(0)/h \end{bmatrix} \in G(1) \end{aligned} \quad (3.14)$$

That is, for any $x(0)$ in $G(2)$, (3.13) forces $x(1)$ into $G(1)$ and is, therefore, the DTOCL for $G(2)$. Again, since in digital implementation, the measurement of x at each sampling instant is treated as an initial state and only $u(0)$ is sought. Thus, the time optimal control law for $G(2)$ can simply be written as

$$u = -\frac{x_2 + y/h}{h}, \left| x_2 + \frac{y}{h} \right| \leq hr; \quad |y| \leq h^2 r \quad (3.15)$$

Remarks:

1. Interestingly, for $\alpha = 0.5$, P is on the straight line c_2c_2 , which bisects $G(2)$ and satisfies $y + hx_2 = 0$. The corresponding control, according to (3.13) is $u(0) = 0$ and it can be shown that the resulting $x(1)$ is in $G(1)$. In other words, for all initial condition $x(0)$ on c_2c_2 , the time optimal control is zero.
2. For the initial condition already in $G(1)$, (3.13) leads to $x(1) = 0$, i.e., the state is driven back to origin in one step.

Now let's consider the DTOCL for the regions beyond $G(2)$ but still bounded by $|x_1 + hx_2| = |y| \leq h^2 r$. These are the areas above $a_{-2}b_2$ and below a_2b_2 but between $y = -h^2 r$ and $y = h^2 r$, which can be expressed as

$$\left| x_2 + \frac{y}{h} \right| > hr; \quad |y| \leq h^2 r \quad (3.16)$$

Here, u continues to take extreme values here, and the DTOCL is

$$u = -r \operatorname{sign}\left(x_2 + \frac{y}{h}\right), \quad \left| x_2 + \frac{y}{h} \right| > hr; \quad |y| \leq h^2 r \quad (3.17)$$

That is, above $a_{-2}b_2$, u continue to take the value of $-r$; below a_2b_2 , it takes r .

Combining (3.13) and (3.17), the DTOCL for the entire area between $y = -h^2 r$ and $y = h^2 r$ is

$$u = -r \operatorname{sat}\left(\left(x_2 + \frac{y}{h}\right), hr\right), \quad |y| \leq h^2 r \quad (3.18)$$

Next, the DTOCL for the area $|y| > h^2 r$ is constructed.

3.3 DTOCL for $|y| \geq h^2 r$

Now let's construct the DTOCL for $G(k)$, $k > 2$, using the same method above. Recall that $G(k)$ are polygons defined as

$$G(k) = \left\{ \sum_{i=1}^k \begin{bmatrix} ih^2 \\ -h \end{bmatrix} u(i-1), |u(i)| \leq r \right\} \quad (2.16)$$

Let

$$a_k = \left\{ \sum_{i=1}^k \begin{bmatrix} ih^2 \\ -h \end{bmatrix} u(i-1), u(i) = r \right\}, \quad (3.19)$$

$$a_{-k} = \left\{ \sum_{i=1}^k \begin{bmatrix} ih^2 \\ -h \end{bmatrix} u(i-1), u(i) = -r \right\}, \quad (3.20)$$

$$b_k = \left\{ \sum_{i=1}^k \begin{bmatrix} ih^2 \\ -h \end{bmatrix} u(i-1), u(0) = r, u(i) = -r \text{ for } i > 0 \right\}, \quad (3.21)$$

$$b_{-k} = \left\{ \sum_{i=1}^k \begin{bmatrix} ih^2 \\ -h \end{bmatrix} u(i-1), u(0) = -r, u(i) = r \text{ for } i > 0 \right\} \quad (3.22)$$

These points, as well as $G(k)$, $k \leq 4$, are shown in Figure 3.2. Clearly,

1. a_k (a_{-k}) are initial conditions from which the state is driven back to the origin by using $u(i)=r$ ($u(i)=-r$), $i=0, \dots, k-1$; furthermore, the broken line connecting $\{a_k, a_{k-1}, \dots, a_1, 0\}$ ($\{a_{-k}, a_{-(k-1)}, \dots, a_{-1}, 0\}$) is the minimum time state trajectory corresponding to $u(i)=r$ ($u(i)=-r$), $i=0, \dots, k-1$;
2. b_k (b_{-k}), $k \geq 2$ are initial conditions from which the state is first driven back to a_{k-1} ($a_{-(k-1)}$) by using $u(0)=-r$ ($u(0)=r$), and then forced to the origin by using $u(i)=r$ ($u(i)=-r$), $i=1, \dots, k-1$;
3. The segments $[b_k a_k]$ ($[b_{-k} a_{-k}]$) are all parallel to $[a_{-1} a_1]$ and their midpoint, c_k (c_{-k}), are initial conditions from which the state is first driven back to a_{k-1} ($a_{-(k-1)}$) by using $u(0)=0$, and then forced to the origin by using $u(i)=r$ ($u(i)=-r$), $i=1, \dots, k-1$;

Connecting $\{\dots, a_k, a_{k-1}, \dots, a_2, b_2, \dots, b_{k-1}, b_k, \dots\}$ forms a boundary denoted as Γ^+ , and $\{\dots, b_{-k}, b_{-(k-1)}, \dots, b_{-2}, a_{-2}, \dots, a_{-(k-1)}, a_{-k}, \dots\}$ Γ^- , as shown in Figure 3.2. Similar to the derivation of DTOCL for $|y| \leq h^2 r$, it can be shown, for $x(0)$ on or above Γ^- (on or below Γ^+), time optimal control calls for $u(0)=-r$ ($u(0)=r$). Moreover, the time optimal control for initial condition inside the area bounded by Γ^+ and Γ^- does not take on extreme values (r or $-r$). In particular, consider $Q=x(0)$ inside a parallelogram defined by $\{a_k, a_{k-1}, b_{-(k-1)}, b_{-k}\}$, $k > 2$, and Q is on a line, $\alpha(b_{-(k-1)}b_{-k}) + (1-\alpha)a_k a_{k-1}$, between and parallel to $a_k a_{k-1}$ and $b_{-(k-1)} b_{-k}$, similar to the P point in $G(2)$ shown in Figure 3.1. The time optimal control is $u(0) = -(2\alpha-1)r$, and it drives $x(1)$ to the segment $[a_{k-2}, a_{k-1}]$. Note that $\alpha=0.5$ corresponds to the broken line connecting $\{\dots, c_k, c_{k-1}, \dots, c_2, c_{-2}, \dots, c_{-(k-1)}, c_{-k}$

$\dots\}$, denoted as Γ^0 , on which the time optimal control is $u(0)=0$.

In summary, the DTOCL is

$$u = \begin{cases} -r & x \text{ is above } \Gamma^- \\ -(2\alpha-1)r & x \text{ is between } \Gamma^- \text{ and } \Gamma^+ \\ r & x \text{ is below } \Gamma^+ \end{cases} \quad (3.23)$$

Remark:

Although this control law can be implemented in a look-up table, a more desirable form is to write u as an explicit function of the state, $x=[x_1 \ x_2]^T$. The first step in achieving this goal is to represent the Γ^- , Γ^0 , and Γ^+ curves as functions of x_1 , x_2 , h , and r .

From the sum of the arithmetic sequences in (3.19) to (3.22), the points that define Γ^- and Γ^+ can be written as

$$a_k = \begin{bmatrix} \frac{k(k+1)h^2 r}{2} \\ -khr \end{bmatrix} = \begin{bmatrix} \frac{x_2^2 - hrx_2}{2r} \\ x_2 \end{bmatrix} \quad (3.24)$$

$$a_{-k} = \begin{bmatrix} \frac{k(k+1)h^2 r}{2} \\ khr \end{bmatrix} = \begin{bmatrix} \frac{x_2^2 + hrx_2}{2r} \\ x_2 \end{bmatrix} \quad (3.25)$$

$$b_k = \begin{bmatrix} \frac{k(k+1)h^2 r}{2} - 2h^2 r \\ -(k-2)hr \end{bmatrix} = \begin{bmatrix} \frac{x_2^2 - 5hrx_2 + 2h^2 r^2}{2r} \\ x_2 \end{bmatrix} \quad (3.26)$$

$$b_{-k} = \begin{bmatrix} -\frac{k(k+1)h^2 r}{2} + 2h^2 r \\ (k-2)hr \end{bmatrix} = \begin{bmatrix} -\frac{x_2^2 + 5hrx_2 + 2h^2 r^2}{2r} \\ x_2 \end{bmatrix} \quad (3.27)$$

Notice that a_i , $i \geq 2$, is on the half-parabola:

$$x_1 = -\frac{hrx_2 - x_2^2}{2r}, \quad x_2 < 0 \quad (3.28)$$

and a_{-i} , $i \geq 2$, is on the half-parabola:

$$x_1 = -\frac{hrx_2 + x_2^2}{2r}, \quad x_2 > 0 \quad (3.29)$$

Let $s = \operatorname{sign}(x_2)$, then $a_{\pm i}$, $i \geq 2$, satisfies

$$x_1 = \frac{-sx_2^2 - hrx_2}{2r} \quad (3.30)$$

Similarly, $b_{\pm i}$, $i \geq 2$, satisfies

$$x_1 = \frac{-s2h^2 r^2 - 5hrx_2 - sx_2^2}{2r} \quad (3.31)$$

Recall that we are interested in the area defined by $|y| \geq h^2 r$, where $y = x_1 + hx_2$. Rewrite (3.30) and (3.31) together as

$$\begin{cases} (x_2 + s \frac{hr}{2} - shr)^2 = \frac{h^2 r^2 - 8rys}{4} = \left(s \frac{\sqrt{h^2 r^2 - 8rys}}{2} \right)^2 \\ (x_2 + s \frac{hr}{2} + shr)^2 = \frac{h^2 r^2 - 8rys}{4} = \left(s \frac{\sqrt{h^2 r^2 - 8rys}}{2} \right)^2 \end{cases} \quad (3.32)$$

which is equivalent to

$$\begin{cases} x_2 - s \frac{\sqrt{h^2 r^2 - 8rys} - hr}{2} = shr, \text{ (connecting } a_{\pm k}) \\ x_2 - s \frac{\sqrt{h^2 r^2 - 8rys} - hr}{2} = -shr, \text{ (connecting } b_{\pm k}) \end{cases} \quad (3.33)$$

Substituting $s = \text{sign}(x_2) = -\text{sign}(y)$, which is valid on the parabolas in (3.33), yields

$$\begin{cases} x_2 + \frac{\sqrt{h^2 r^2 - 8rys} - hr}{2} \text{sign}(y) = -hr \text{sign}(y), \text{ (connecting } a_{\pm k}) \\ x_2 + \frac{\sqrt{h^2 r^2 - 8rys} - hr}{2} \text{sign}(y) = hr \text{sign}(y), \text{ (connecting } b_{\pm k}) \end{cases} \quad (3.34)$$

Define

$$a(x_1, x_2, r, h) = x_2 + \frac{\sqrt{h^2 r^2 - 8rys} - hr}{2} \text{sign}(y), \quad |y| \geq h^2 r \quad (3.35)$$

then $a(x_1, x_2, r, h) = -hr$ corresponds to the parabolas connecting a_k and b_k , respectively, and this curve, denoted as $\tilde{\Gamma}^+$, overlaps Γ^- at the points $\{a_{-k}, b_{-k}, k = 2, 3, \dots\}$. Similarly, $a(x_1, x_2, r, h) = hr$ corresponds to the parabolas connecting a_k and b_k , respectively, and this curve, denoted as $\tilde{\Gamma}^-$, overlaps Γ^+ at the points $\{a_k, b_k, k = 2, 3, \dots\}$. It can also be shown that $a(x_1, x_2, r, h) = 0$ represents $\tilde{\Gamma}^0$, which overlaps Γ^0 at the points $\{c_{\pm k}, k = 2, 3, \dots\}$. Moreover, $\tilde{\Gamma}^+$ and $\tilde{\Gamma}^-$ partition the phase plane in a manner of

$$\begin{cases} a(x_1, x_2, r, h) \leq -hr, x = [x_1, x_2]' \text{ is below } \tilde{\Gamma}^+ \\ a(x_1, x_2, r, h) \geq hr, x = [x_1, x_2]' \text{ is above } \tilde{\Gamma}^- \\ |a(x_1, x_2, r, h)| \leq hr, x = [x_1, x_2]' \text{ between } \tilde{\Gamma}^- \text{ and } \tilde{\Gamma}^+ \end{cases} \quad (3.36)$$

from which the DTOCL of (3.23) is approximated, with very little error because $\tilde{\Gamma}^+$ and $\tilde{\Gamma}^-$ are generally very close to Γ^+ and Γ^- , as

$$u = -rsat(a(x_1, x_2, r, h), hr), \quad |y| \geq h^2 r \quad (3.37)$$

Combining (3.18) and (3.37), and redefine $a(x_1, x_2, r, h)$ as

$$a(x_1, x_2, r, h) = \begin{cases} x_2 + \frac{\sqrt{h^2 r^2 - 8rys} - hr}{2} \text{sign}(y), & |y| > h^2 r \\ x_2 + y/h, & |y| \leq h^2 r \end{cases} \quad (3.38)$$

the complete DTOCL for any initial condition on the x_1 - x_2 plane is

$$u = -r \text{sat}(a(x_1, x_2, r, h), hr) \quad (3.39)$$

which can then be coded in a digital computer as in (3.40).

$$\begin{cases} u = \text{fst}((x_1, x_2, r, h)) \\ d = rh; d_0 = hd \\ y = x_1 + hx_2 \\ a_0 = \sqrt{d^2 + 8r|y|} \\ a = \begin{cases} x_2 + \frac{a_0 - d}{2} \text{sign}(y), & |y| > d_0 \\ x_2 + y/h, & |y| \leq d_0 \end{cases} \\ \text{fst} = \begin{cases} r \text{sign}(a), & |a| > d \\ r \frac{a}{d}, & |a| \leq d \end{cases} \end{cases} \quad (3.40)$$

3.4 Characteristics of the Switching Surfaces

The switching curves of the original continuous TOC and the newly derived DTOCL are shown together in Figure 3.3, with $h=1$ and $r=2$. It is interesting to note that the original TOC stays within the area between Γ^- and Γ^+ in the neighborhood of the origin but deviates from it as $x(0)$ ventures further away. That is, the switching curve of the original TOC is a solution for the DTOC problem.

IV. CONCLUDING REMARKS

A discrete time optimal control law is derived for a double-integral plant. A closed-form solution is obtained, which is ready for implementation in any digital control platform. This new time optimal control law resolves the long standing issue of chattering in the control signal and is, therefore, much more practical than the well-known bang-bang control solution. The readers are referred to [10,11,14,15,17] for more details of the applications.

ACKNOWLEDGEMENT

The author thanks Prof. Jingqing Han for his unselfishness in sharing his vision and methods with us, and Cheng Gao for his assistance in verifying the arithmetic in derivations.

REFERENCES

- [1] A. M. Hopkin, "A Phase Plane Approach to the Design of Saturating Servomechanisms," Trans. AIEE, vol. 70, pp. 631-639, 1950.
- [2] D.C. McDonald, "Nonlinear Techniques for Improving Servo Performance," Proc. Natl. Electron. Conf., vol. 6, pp. 400-421, 1950.
- [3] D.W. Bushaw, "Differential Equations with a Discontinuous Forcing Term," Stevens Institute of Technology Experimental Towing Tank Report 469, Hoboken, N.J., January 1953.
- [4] L.S. Pontryagin, V.G. Boltyanskii, R.V. Gamkrelidze, and E.F. Mishchenko, *The Mathematical Theory of Optimal Processes*, Interscience Publishers, Inc. New York, 1962.
- [5] M. Athans and P. Falb, *Optimal Control*, McGraw-Hill Book Company, New York, 1966.
- [6] D.E. Kirk, *Optimal Control Theory*, Prentice Hall, 1970.

- [7] H.S. Tsien and Jian Song, *Engineering Cybernetics*, Science Press, 1980 (Chinese).
- [8] Sun Jian and Hang King-Ching, "Analysis and Synthesis of Time Optimal Control Systems," Proc. of the Second IFAC Congress, Basel, 1963.
- [9] Sun Jian, Hang King-Ching, and Tang Zhiqiang, "Time Optimal Control Synthesis for Linear Time Invariant Systems with Discontinuities," Proc. Of the Conference of Ordinary Differential Equations, Beijing, 1965.
- [10] J. Han and L. Yuan, "The Discrete Form of the Tracking Differentiator," *Systems Science and Mathematical Sciences*, vol.19, no.3, pp.268-273, 1999. (In Chinese)
- [11] J. Han and W. Wang, "Nonlinear Tracking Differentiator," *Systems Science and Mathematical Sciences*, vol.14, no. 2, pp.177-183, 1994. (In Chinese)
- [12] M. Muenchhof and T. Singh, "Jerk Limited Time Optimal Control of Multi-input Systems," Proc. of the American Control Conference, Anchorage, AK, pp. 328-333, May 8-10, 2002.
- [13] S. K. Lucas and C. Y. Kaya, "Switching-Time Computation for Bang-Bang Control Laws," Proc. of the American Control Conference, Arlington, VA, pp. 176,181, June 25-27, 2002.
- [14] Z. Gao, Y. Huang, and J. Han, "An Alternative Paradigm for Control System Design," presented at the 40th IEEE Conference on Decision and Control, Dec 4-7, 2001, Orlando, Florida.
- [15] Z. Gao, "From Linear to Nonlinear Control Means: A Practical Progression," *ISA Transactions*, vol.41, no.2 p. 177-89, April 2002.
- [16] Z. Gao, "Scaling and Parameterization Based Controller Tuning," Proc. of the 2003 American Control Conference, pp. 4989-4996, June 2003.
- [17] Z. Gao, "On Discrete Time Optimal Control: Applications", Submitted for publications.

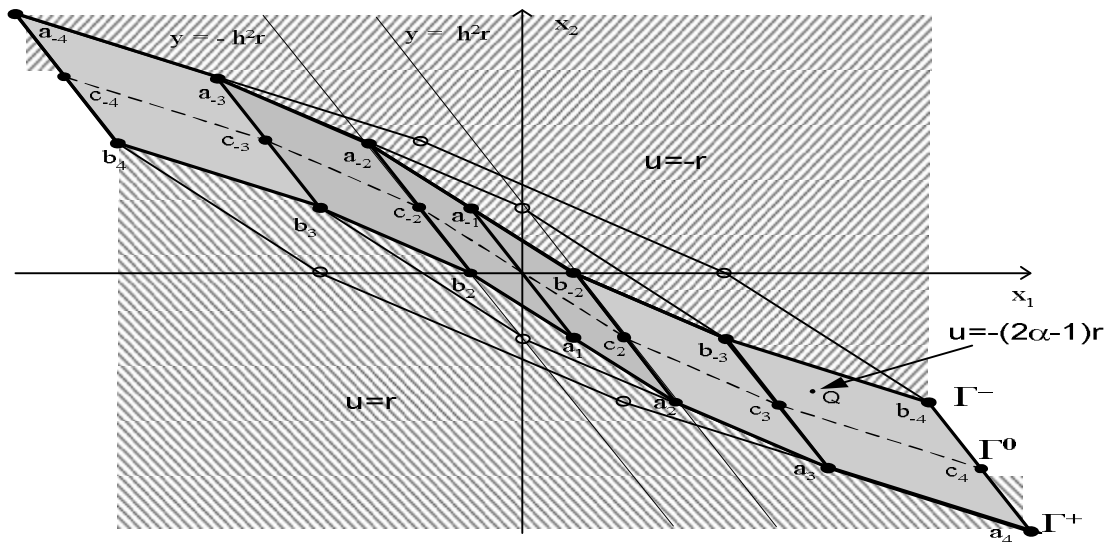


Figure 3.2 Switching surface for DTOCL

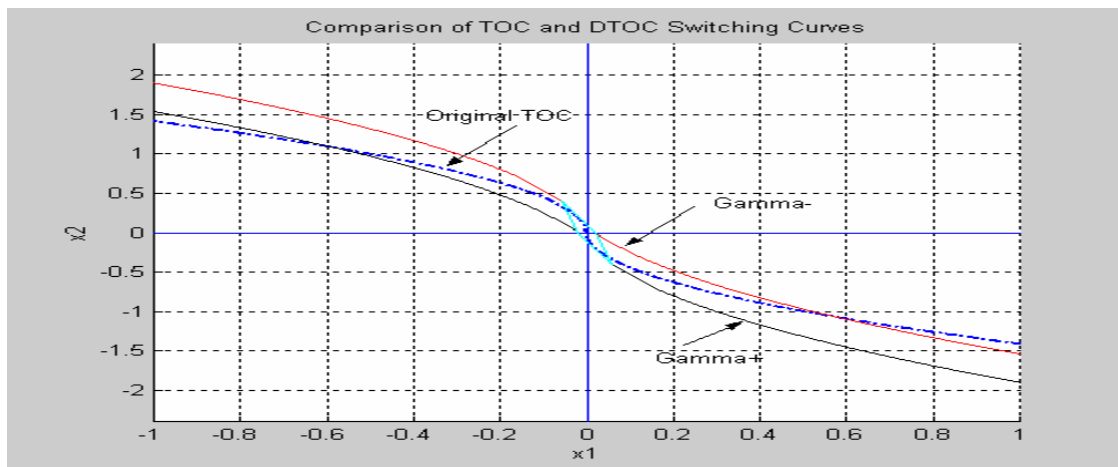


Figure 3.3 Comparison of switching curves